Article:
Ubellacker, J.M., Baryawno, N., Severe, N. et al. (13 more authors) (2018) Modulating bone marrow hematopoietic lineage potential to prevent bone metastasis in breast cancer. Cancer Research . ISSN 0008-5472

https://doi.org/10.1158/0008-5472.CAN-18-0548

Modulating bone marrow hematopoietic lineage potential to prevent bone metastasis in breast cancer

Jessalyn M. Ubellacker[1,2], Ninib Baryawno[3,4,5], Nicolas Severe[3,4,5], Molly J. DeCristo[1,2], Jaclyn Sceneay[1,2], John N. Hutchinson[6], Marie-Therese Haider[7], Catherine S. Rhee[3,4,5], Yuanbo Qin[1,2], Walter M. Gregory[8], Ana C. Garrido-Castro[9], Ingunn Holen[7], Janet E. Brown[7], Robert E. Coleman[7], David T. Scadden[3,4,5,10], Sandra S. McAllister[1,2,5,10]

[1]Hematology Division, Brigham & Women's Hospital, Boston, Massachusetts, 02115, USA.
[2]Department of Medicine, Harvard Medical School, Boston, Massachusetts, 02115, USA.
[3]Department of Stem Cell and Regenerative Biology, Harvard University, Cambridge, Massachusetts, 02138, USA.
[4]Center for Regenerative Medicine and the Cancer Center, Massachusetts General Hospital, Boston, Massachusetts, 02114, USA.
[5]Harvard Stem Cell Institute, Cambridge, Massachusetts, 02138, USA.
[6]Department of Biostatistics, Harvard T.H. Chan, School of Public Health, Boston, Massachusetts, 02115, USA.
[7]Academic Unit of Clinical Oncology, Department of Oncology & Metabolism, Weston Park Hospital, University of Sheffield, Sheffield, UK, S10.
[8]Clinical Trials Research Unit, University of Leeds, Leeds, UK, LS2 9NL.
[9]Department of Medical Oncology, Dana-Farber Cancer Institute, Boston, Massachusetts, 02115, USA.
[10]Broad Institute of Harvard and MIT, Cambridge, Massachusetts, 02142, USA.

Corresponding author: Sandra S. McAllister, (+01) 617-525-4929, smcallister1@bwh.harvard.edu

Running title: Modulating bone marrow to prevent breast cancer metastasis

Keywords: breast cancer, bone metastasis, hematopoiesis, bone marrow, myeloid cells, myeloid/osteoclast progenitors, bisphosphonate, zoledronic acid, granulocyte-colony stimulating factor

Conflict of interest disclosure: Robert E. Coleman has participated in a consultant/advisory board relationship with Amgen, has leadership affiliation with prIME Oncology, and has ownership interests in Inbiomotion. Janet E. Brown has participated in a consultant/advisory board relationship with and has received honoraria from Amgen and Novartis. All other authors have declared that no conflict of interest exists.

Financial Support: This work was supported by funds from NIH T32 GM007226, NIH NCI F31CA195797 for J. Ubellacker; NIH R01DK107784, NIH NCI U54CA163191 to D. Scadden; U.S. Department of Defense Era of Hope W81XWH-14-1-0191, NIH NCI RO1 CA166284 with PECASE supplemental to S. McAllister.

Word count: 6,994
Number of figures: 7

ABSTRACT

The presence of disseminated tumor cells in breast cancer patient bone marrow aspirates predicts decreased recurrence-free survival. Although it is appreciated that physiological, pathological, and therapeutic conditions impact hematopoiesis, it remains unclear if targeting hematopoiesis presents opportunities for limiting bone metastasis. Using pre-clinical breast cancer models, we discovered that marrow from mice treated with the bisphosphonate zoledronic acid (ZA) are metastasis-suppressive. Specifically, ZA modulated hematopoietic myeloid/osteoclast progenitor cell (M/OCP) lineage potential to activate metastasis-suppressive activity. Granulocyte-colony stimulating factor (G-CSF) promoted ZA resistance by redirecting M/OCP differentiation. We identified M/OCP and bone marrow transcriptional programs associated with metastasis suppression and ZA resistance. Analysis of patient blood samples taken at random revealed that women with high plasma G-CSF experienced significantly worse outcome with adjuvant ZA than those with lower G-CSF levels. Our findings support discovery of therapeutic strategies to direct M/OCP lineage potential and biomarkers that stratify responses in patients at risk of recurrence.

STATEMENT OF SIGNIFICANCE

Bone marrow myeloid/osteoclast progenitor cell (M/OCP) lineage potential has a profound impact on breast cancer bone metastasis and can be modulated by G-CSF and bone-targeting agents.

INTRODUCTION

The majority of breast cancer patients have no evidence of metastatic disease at the time of diagnosis, yet ~30% of patients experience recurrent breast cancer in the form of metastasis, of which the most prominent site is bone (1). Moreover, bone is the most frequent site of de novo metastasis for all breast cancer molecular subtypes (2). At present, little is known about what promotes tumor cell survival and outgrowth into incurable disease in the bone (1, 3). Disseminated tumor cells (DTCs) are frequently detected in bone marrow aspirates of breast cancer patients, regardless of breast cancer subtype and even in those who have early-stage disease, and are predictive of decreased recurrence-free survival (4). These and other such findings support the idea that DTCs find a hospitable niche in the bone marrow (4-6).

Bone metastatic niches in which DTCs reside have been defined as microdomains within the bone that support tumor cell seeding and outgrowth and are predominantly comprised of hematopoietic cells, mesenchymal stromal cells, osteoblasts, osteoclasts, and/or vascular cells (5, 6). Paracrine interactions between DTCs and these various stromal cells disrupt bone homeostasis, which is normally tightly controlled, to fuel metastatic progression. For example, it is well established that DTCs secrete a variety of cytokines that promote osteoclast activity, which in turn, causes release of a variety of tumor-promoting growth factors from the bone, thus propagating a vicious cycle of tumor outgrowth and osteolytic bone breakdown (6).

Although results from studies that focused on mesenchymal stromal cells, osteoblasts, osteoclasts, and vascular cell activity have yielded significant insights into cellular and molecular processes that influence DTC outgrowth and dormancy in the

bone (5, 6), surprisingly little is known about whether or how hematopoietic cells in the marrow compartment impact bone metastases. Clinical studies indicate that the presence of DTCs in breast cancer patient bone marrow correlates with metastatic relapse and poor outcome (7). In the pre-clinical setting, it is becoming increasingly apparent that various physiological and pathological processes as well as certain drugs and chemotherapies alter hematopoietic cells in the marrow in ways that impact cancer progression (7-10); however, it is not yet clear how DTCs are impacted when they first encounter such hematopoietic cells in the marrow.

Hematopoiesis relies on precise regulation of quiescence, proliferation, and differentiation of hematopoietic progenitor cells within specialized niches (11, 12). For example, within the osteoblastic niche, mature osteoclasts influence hematopoiesis by releasing bone-matrix proteins essential for hematopoietic cell maintenance (13, 14). It is reasonable therefore to hypothesize that modulating osteoclast (OC) activity would have an impact on hematopoiesis in ways that affect DTC behavior.

We previously established that bisphosphonate treatment, which is a widely used osteoclast inhibitor therapy for effective treatment of osteolytic diseases, induces sub-clinical changes in the composition of bone marrow hematopoietic progenitor populations (15). We reported that bone marrow cells isolated from ZA-treated animals suppress mammary carcinoma formation in the absence of a direct effect of ZA on tumor cells, indicating that the bone marrow harbors the majority of ZA's tumor-suppressive capacity (15). However, whether such modulation of the marrow affects breast cancer bone metastasis independently of the effects on mature osteoclasts in the endosteal niche and whether a specific subpopulation of hematopoietic cells has

metastasis-suppressive capacity remained undetermined. A better understanding of the bone marrow microenvironment and processes that influence tumor cell maintenance and growth in the bone should present opportunities for targeting hematopoietic cell populations as part of anti-cancer therapy.

MATERIALS AND METHODS

Cell lines. MDA-MB-231 B1 cells (gift from Dr. Gabri van der Pluijm), a clonal bone-tropic human breast cancer cell line expressing luciferase, was maintained under selection in 1 mg/mL Gentamicin, (G418, Life Technologies, 15750060) in Dulbecco modified Eagle medium (DMEM) with 10% fetal bovine serum (FBS). MDA-MB-231 B2 bone-tropic human breast cancer cells (gift from Dr. Penelope Ottewell were transfected with luciferase and maintained in 10% FBS in DMEM. Cells were not used beyond passage five post thawing. All cells tested negative for mycoplasma (Lonza Kit: LT07-118) every 6 months (Last test: June 2017) and were validated using short tandem repeat (STR) profiling (Molecular Diagnostics Laboratory at Dana-Farber Cancer Institute, Boston, MA).

Mice. Six to seven-week-old female CrTac:NCr-*Foxn1*^{nu} (nude) female mice were purchased from Taconic Laboratories (Hudson, NY). C57BL/6J female mice were purchased from The Jackson Laboratory (Bar Harbor, ME). All animal procedures were performed in accordance with the ethics and regulations of Brigham & Women's Hospital Institutional Animal Care and Use Committee (protocol approval 2017N000056), Boston Children's Hospital Institutional Animal Care and Use

Committee (protocol approval 12-11-2308R), and Massachusetts General Hospital (protocol approval 2017N000023).

Drug administration. Zoledronic acid (ZA) [1-hydroxy-2-(1H-imidazole-1-yl)ethylidene-bisphosphonic acid] (Novartis Pharmaceuticals, Cambridge, MA) was dissolved in 1X Hank's Balanced Buffer Solution (Gibco) and stored at 4°C until use. ZA was administered to mice at a dose of 100 μg/kg (i.p.). Recombinant human granulocyte colony stimulating factor (G-CSF) (carrier-free, Biolegend #578604) was administered to nude mice each day for 3 days at a dose of 50 μg/kg (i.p.) beginning one day after administration of ZA, and C57BL/6 mice each day for 3 days at a dose of 50 μg/kg (i.p.) beginning 2 days after administration of ZA. For G-CSF depletion experiments, nude mice were treated with 100 μg/kg (i.p.) G-CSF antibody (R&D Systems, MAB414100) or the 100 μg/kg (i.p.) isotype control IgG (R&D Systems, MAB005) six hours prior to intracardiac injection of tumor cells.

Blood and plasma. At experimental end points, blood was collected by intracardiac puncture with a 27-gauge needle into ethylenediaminetetraacetic acid (EDTA) Microtainer tubes (BD Pharmingen). Complete blood counts were obtained using a HEMAVET® hematology analyzer (Drew Scientific). Plasma was prepared by centrifugation of whole blood at 1.5 g x 1000 for 8 minutes at 4 °C.

Experimental bone metastasis. Mice were anesthetized with isoflurane, and $1x10^5$ luciferase-tagged bone-tropic cell lines (B1, B2, B1-G, B2-shG) were suspended in 100 μL of PBS and injected into the left cardiac ventricle. Tumor growth was monitored by

bioluminescence imaging, and by Vybrant® CM-DiI cell-labeling solution by florescence imaging (Life Technologies, V22888). For intratibial injections, mice were anesthetized with isoflurane and $5x10^4$ cells in 10 µL of PBS were injected directly into both tibiae. Tumor growth was monitored by bioluminescence imaging. In indicated experiments, mice were treated with 100 µg/kg of ZA or equivalent volume of vehicle control 72 hours prior to injection of tumor cells.

Bone marrow cell preparations. Femora and tibiae were dissected free into 2% FBS in PBS and centrifuged at 6.0-7.0 g x1000 for 4 minutes at 4 °C to collect whole BMCs (WBM). Cells were then incubated with red blood cell (RBC) lysis solution (BioLegend, 420301) for 5 minutes on ice, washed once with 2% FBS in PBS, re-suspended in 0.5 mL of sterile BMC buffer, and passed through a 5-mL polystyrene round-bottom tube with a cell-strainer cap (Corning, 352235).

Flow cytometry and FACS. BMCs were prepared for flow cytometry by suspension in sterile PBS containing 2% FBS. Cells were labeled with appropriate antibodies for 30 minutes at 4°C. Gating was used to exclude debris, cell clumps, and dead cells (using 7-aminoactinomycin D; 7-AAD Viability Staining Solution (BioLegend, 420404). Myeloid/osteoclast progenitor cell (M/OCP) populations were defined as Lineage-CD115+. Antibody panel includes: Pacific Blue™ anti-mouse Lineage Cocktail (BioLegend, 133310: CD3-, Ly-6G/Ly6-C-, Cd11b-, CD45R-, TER119-) and Alexa Fluor® 488 anti-mouse CD115 (CSF-1R; BioLegend, 135511). Cells were acquired on a Canto II or a FACSAria IIu/FACSDiva (BD Biosciences). At the endpoint of the

osteoclast differentiation assays, macrophages were defined as MHCII+/F4/80+/Cd11b+ (MHCII: APC-Cy7 (BioLegend 107627), F4/80: PE-Cy-7 (BioLegend 123113), Cd11b:Alexa Fluor-488 (BioLegend 101205)) and dendritic cells were defined as MHCII+/Cd11b+/Cd11c+ (MHCII: APC-Cy7 (BioLegend 107627), Cd11c: PE (BioLegend 117307), Cd11b:Alexa Fluor-488 (BioLegend 101205)). Analyses were performed using FlowJo software (FlowJo, LLC). CountBright ™ Absolute Counting Beads (Life Technologies, C36950) were used to quantify absolute cell numbers. For cell sorting of the M/OCP populations and for isolation of Lin- and Lin+ populations, the Murine Direct Lineage Cell Depletion Kit (Miltenyi Biotec Inc., 130-110-470) was used to enrich for Lin- populations, which was confirmed by flow cytometry for the markers in the lineage cocktail.

Bone marrow tumor support functional assay. Donor mice were treated via i.p. injection with vehicle (1X HBBS) or ZA (100ug/kg) and sacrificed 3 days (nude mice) or 5 days (C57BL/6 mice) following treatment. BMCs were harvested as described above. For whole bone marrow (WBM) assays, 750,000 donor BMCs were mixed with 250,000 of the appropriate tumor cells in 100uL DMEM with 10% Basement membrane matrix, Corning™ Matrigel Growth Factor Reduced (Low Growth) (Westnet Inc., 354230) immediately prior to injection. To test the tumor support function of various FACS-isolated marrow subpopulations, 250,000 tumor cells were mixed with either 250,000 Lin- BMCs, 750,000 Lin+ BMCs, or 100,000 M/OCPs. Admixtures were injected subcutaneously into host nude mice. During the 14-day time courses, no graft versus host disease was observed for nude mice receiving C57BL/6 donor marrow. Each donor

BMC sample was distributed into a minimum of 3 host nude mice. Tumor growth was monitored by bioluminescent imaging.

Osteoclast differentiation assay. Bone marrow cells were prepared as previously described, and 1,000 WBM cells or 250 M/OCP cells were plated in 24-well plates with 15% FBS in αMEM with 10 ng/mL of Recombinant M-CSF (R&D Systems, 416ML010). After 3 days, recombinant RANKL (5 ng/mL R&D Systems, 462TEC010CF) or vehicle control were added to the assay. At the 5-day end point, Tartrate Resistant Acid Phosphatase, Leukocyte (TRAP) Kit (Sigma Aldrich, 387A) was used and TRAP-positive osteoclasts were counted and flow cytometry was performed to quantify the numbers of macrophages and dendritic cells in the resultant cultures. To test phagocytic function of the resulting cultures, tumor cells were stained with Vibrant CM-DiI (Life Technologies) at a concentration of 5 µL CM-DiI solution per 1 million cells/mL for 5 minutes at 37 degrees. Cells were washed twice with PBS, and then 1,000 tumor cells were added into the wells at the endpoint of the osteoclast differentiation assay. After two hours, wells were washed with PBS and prepared for flow cytometry. Cells within the macrophage gate that were CM-DiI+ were reported as a percentage of the total macrophage population.

Patient plasma samples. Breast cancer patient plasma samples (n=392) were obtained from the AZURE clinical trial sample database (ISRCTN79831382, University of Sheffield) (16). The AZURE study was performed in accordance with the Declaration of Helsinki, and was performed after approval by an institutional review board (IRB) (West Midlands Research Ethics Committee). Patients were randomized to either

standard adjuvant therapy alone (Ctl) or with zoledronic acid (ZA) (Novartis Pharmaceuticals, Summit, New Jersey, USA) and written informed consent was received from all patients prior to inclusion in the study. To reduce possible imbalances in tumor and treatment characteristics, a minimization process was used that took into account the number of involved axillary lymph nodes, clinical tumor stage, estrogen receptor status, type and timing of systemic therapy, menopausal status, statin use and treating center. Eligible patients were randomized to receive (neo) adjuvant chemotherapy and/or endocrine therapy +/- ZA 4mg iv every 3-4 weeks for 6 doses, then 3 monthly x8 and 6 monthly x5 to complete 5 years of treatment. Secondary prophylaxis with G-CSF to prevent neutropenic sepsis or treatment delays due to neutropenia was allowed but primary G-CSF prophylaxis was not used. Both the use of adjuvant systemic treatments and loco-regional radiotherapy were given in accordance with standard protocols at each participating institution. The date of recurrence was defined as the date on which relapse was first suspected. Subjects were followed up on an annual basis after completion of the 5-year treatment phase (ZA or Ctl) for both disease and relevant safety endpoints (16). Patient samples to be used in this study were selected based on: 1.) menopausal status (post-menopausal women (n=164); non-postmenopausal women (n=226); unknown menopausal status (n=2)), 2.) whether or not the patient had recurrence of breast cancer (disease-free or recurrence in bone only or bone as well as other distant sites), and 3.) whether or not the patient received adjuvant ZA treatment. These three parameters were used to power the sample size estimation using the reported HR of 0.81, and a standardized effect size of 0.80 (16). Plasma G-CSF levels were analyzed by ELISA.

Statistics. All experiments were performed with three independent replications, unless otherwise indicated. Sample size for *in vivo* experiment was based on outcomes from pilot experiments and was calculated at a statistical significance level of 0.05, and powered at 0.80. All data were analyzed with the use of GraphPad Prism Software (Version 7). Data are expressed as mean ± SEM with n denoting the number of independent data points (i.e., mice, cell wells, etc.). Statistics were determined using the unpaired, two-tailed student's t-test unless otherwise indicated. Results were considered statistically significant if $p<0.05$ (*), $p<0.01$ (**), $p<0.001$ (***).

ELISAs and cytokine array. Plasma was obtained from the mice as previously described, and ELISA assays were performed according to manufacturer instructions: Murine G-CSF ELISA Kit (R&D Systems, MCS00); Murine OPG ELISA Kit (Raybiotech Inc., 501044763); Murine RANKL ELISA Kit (Innovative Research, IRKTAH5466); Murine NTX ELISA (Biotang Inc., 50154363). For the human cytokine array, 100,000 cells of B1 or B2 were plated and conditioned media from 5 different wells was obtained 24 hours after plating, was pooled and then assessed using Human Cytokine Array, Panel A per manufacturer's instructions (R&D, ARY005). For the patient plasma samples, 100 µL of sample was used and ELISA assays were performed according to manufacturer instructions (Human G-CSF QKIT HS ELISA; R&D Systems, HSTCS0). Plates were analyzed using Softmax Pro7 Software (Molecular Devices).

DATA AND SOFTWARE AVAILABILITY. RNA-Sequencing data will be available using the Gene Expression Omnibus (GEO; GSE108250) database.

RESULTS

Identification of therapeutically induced tumor-inhibitory hematopoietic bone marrow cells

We and others have reported that primary cancers, physiological aging, and drug treatments all affect bone marrow hematopoietic cells in ways that influence disease progression (8-10, 15, 17). To understand if therapeutic modulation of the bone marrow microenvironment would provide an effective approach for treating breast cancer bone metastasis, we used the nitrogen-containing bisphosphonate, zoledronic acid (ZA) in both immunocompromised and immunocompetent pre-clinical models of breast cancer.

We treated tumor-free cohorts of C57BL/6 and nude mice with a single dose of either ZA or vehicle control and harvested their bone marrow 5 days (C57BL/6 mice) or 3 days (nude mice) following treatment. These are time points at which osteoclast activity is inhibited by ZA (15). We then used our well-established hematopoietic cell functional assay (15-18) to test the bone marrow for effects on growth of a bone-metastatic human breast tumor cell line, MDA-MB-231-B1 (B1), (Figure 1A). This assay is designed to test any effects on tumor growth that are exclusively mediated by bone marrow hematopoietic cells and is based on the notion that the outgrowth of DTCs would be affected by any ZA-induced changes to hematopoietic cells. Importantly, mature osteoclasts are of hematopoietic origin but localize to the endosteal niche upon maturation (19). TRAP staining of the bone marrow plugs confirmed that osteoclasts were absent from the bone marrow samples used in these experiments (Supplemental Figure S1A).

Whole bone marrow (WBM) from both strains of control (Ctl)-treated donor mice had no significant effect on subcutaneous B1 tumor growth when compared with B1 tumor cells injected alone – in these cohorts, tumors formed with ~80% incidence in both strains of mice (Figure 1B, Supplemental Figure S1B). However, WBM from both strains of ZA-treated mice significantly reduced B1 tumor incidence to <30% (Figure 1B, Supplemental Figure S1B), indicating that tumor suppression occurred independently of a functional adaptive immune system.

To begin to understand if tumor-suppressive function is enriched in a particular subpopulation of hematopoietic cells, we sorted the marrow from Ctl or ZA treated mice into lineage-negative (Lin-) progenitor populations and mature lineage-positive (Lin+) populations and assessed B1 tumor growth using the bone marrow functional assay. As before, WBM from the ZA-treated mice suppressed B1 tumor formation; tumor incidence was only 50% of that from the respective Ctl cohort (Figure 1C). The Lin+ subpopulation from ZA-treated mice had no effect on tumor incidence, which was equivalent to that of the respective Ctl subpopulation (Figure 1C). In striking contrast, Lin- cells from ZA-treated donors significantly reduced B1 tumor incidence to only 14.3% relative to Lin- cells from the Ctl mice (Figure 1C).

Osteoclasts differentiate from Lin- myeloid-committed cells in the marrow (19-21); therefore, we wondered if ZA imparted its tumor-suppressive effect via osteoclast precursor cells. There is currently no clear consensus on the cell-surface markers that delineate osteoclast precursors (21). However, given our previous report that ZA, in addition to inhibiting osteoclast activity, significantly expands numbers of bone marrow common myeloid progenitor populations (15), we reasoned that an effort to capture

functional activity should include multi-potent progenitors of the myeloid/osteoclast lineage. We therefore utilized the markers $CD3^-B220^-Ly6G^-Ly6C^-CD11b^-Ter119^-CD115^+$ to define a population we termed 'myeloid/osteoclast progenitors' (M/OCPs; Supplemental Figure S1C). We confirmed that this sorted population from Ctl-treated donors gives rise to macrophages, dendritic cells, and osteoclasts in a standard *in vitro* differentiation assay (20) (Supplemental Figure S1D, S1E).

We treated tumor-free C57BL/6 mice with a single dose of ZA and quantified the numbers of $CD3^-B220^-Ly6G^-Ly6C^-CD11b^-Ter119^-CD115^+$ M/OCPs in the marrow over an experimental time course of 15 days. ZA treatment significantly increased the number of bone marrow M/OCPs in a time-dependent manner (Figure 1D).

We then investigated M/OCP tumor-suppressive function by sorting $CD3^-B220^-Ly6G^-Ly6C^-CD11b^-Ter119^-CD115^+$ M/OCPs, as well as the M/OCP-depleted population, from the marrow of Ctl or ZA-treated cohorts and subjecting them to the bone marrow functional assay. As a control, we confirmed that WBM from the ZA-treated cohort significantly suppressed tumor growth as expected (Figure 1E, Supplemental Figure S1F). M/OCPs isolated 5 days after ZA-treatment significantly inhibited tumor incidence and mass relative to the same number of M/OCPs from the Ctl-treated cohort (Figure 1E, Supplemental Figure S1F). In contrast, the M/OCP-depleted marrows from Ctl and ZA-treated mice were not significantly different in their tumor-modulating capacity (Figure 1E).

The results from the *in vivo* BMC functional assays suggested that M/OCPs from ZA-treated mice are qualitatively different than their control counterparts. Hence, we performed RNA sequencing on M/OCPs from Ctl and ZA-treated cohorts.

Computational analyses revealed a list of significantly differentially expressed genes (DEGs) (GEO, GSE108250; Supplemental Table S1). Functionally enriched gene ontology (GO) terms and gene set enrichment analyses (GSEA) among the DEGs revealed biological and cellular processes that were enriched in the ZA-treated M/OCPs. Of these, “organic cyclic compound metabolic process”, “cellular aromatic compound metabolic process”, “oxidative phosphorylation”, “phagosome”, “lysosome organization”, and “lipid transport” pathways (Figure 1F, Supplemental Table S2A, S2B) were particularly interesting, as these processes are important for monocyte differentiation and macrophage function (22, 23).

Collectively, these results established that M/OCP transcriptional programs are altered in the marrow and correlate with tumor-suppressive function in response to the bone-targeting agent, ZA, independently of a functional adaptive immune system. Moreover, these results are in agreement with pre-clinical findings that ZA reduces the risk of breast cancer recurrence independently of its direct action on osteoclast apoptosis (24) and that bone tumor burden can be modulated in an osteoclast-independent manner (25).

ZA skews lineage potential of myeloid/osteoclast progenitor cells toward macrophages

Our RNAseq analyses suggested that M/OCPs are enriched for transcriptional programs consistent with those of the monocyte/macrophage lineage in response to ZA. Although it is well known that ZA inhibits mature osteoclasts, whether ZA affects myeloid/osteoclast lineage bias is not understood; therefore, we tested the lineage

potential of bone marrow samples from control and ZA-treated mice using *in vitro* differentiation assays (20) (Figure 2A). In these assays, macrophage-colony stimulating factor (M-CSF; CSF1) is necessary for sustaining M/OCP populations (26) and in the absence of receptor activator of nuclear factor kappa-B ligand (RANKL), these progenitors normally differentiate into macrophages and dendritic cells (DCs) whereas in the presence of RANKL, they differentiate into osteoclasts (27).

Interestingly, when WBM samples from ZA- and Ctl-treated mice were subjected to M-CSF and RANKL *in vitro*, the marrow cells from ZA-treated donors gave rise to significantly fewer numbers of osteoclasts as compared to those of Ctl-treated donors (Figure 2B), despite having more M/OCPs (Figure 1D). Instead, the resulting cultures from the ZA-treated cohort had significantly increased numbers of macrophages ($Cd11b^+/F4/80^+/MHCII^+$) and DCs ($Cd11b^+/MHCII^+/Cd11c^+$) as compared to those of the Ctl-treated cohort (Figure 2C; Supplemental Figure S2A, S2B). In fact, these numbers of macrophages and DCs were comparable to those of bone marrow samples treated only with M-CSF (Figure 2C).

We next tested the lineage potential of M/OCPs isolated from ZA-treated animals. Thus, we sorted M/OCP populations from the marrow of mice treated with Ctl or ZA and subjected them to the differentiation assay. In the presence of RANKL, M/OCPs from ZA-treated mice gave rise to significantly more macrophages than those of controls and these numbers were comparable to those from cultures that had not been treated with RANKL (Figure 2D). Although DCs were detected in the resulting cultures, there were no significant differences in their numbers between ZA and Ctl treated mice (Figure 2D, Supplemental Figure S2B).

Collectively, these findings indicated that ZA inherently changes the lineage potential of M/OCPs by skewing their differentiation potential toward macrophages, even in the presence of RANKL. Moreover, the marrow of ZA-treated cohorts harbor significantly more of these differently poised M/OCPs than that of the control counterparts.

ZA inhibits breast cancer metastasis in a manner that is counteracted by G-CSF

The ability to therapeutically generate tumor-suppressive bone marrow has important implications for bone metastasis; therefore, we tested whether pre-treating nude mice with ZA three days prior to intracardiac injection of breast tumor cells would affect subsequent bone metastasis (Figure 3A). We used two derivative bone-tropic subpopulations, B1 (28) and B2 (29), of the parental MDA-MB-231 breast cancer cell line.

Interestingly, while B1 bone metastatic burden was significantly lower following ZA pre-treatment (63.7% lower than the control cohort, $p<0.05$), B2 metastatic burden was unaffected (Figure 3B-C; Supplemental Figure S3A). Likewise, ZA pre-treatment decreased outgrowth of B1, but not B2, bone tumors when cells were directly injected into the tibia (Supplemental Figure S3B). Moreover, WBM from ZA-treated mice did not suppress B2-derived tumor growth in the BM functional assay (Supplemental Figure S3C), indicating that the B2 cell line is resistant to the tumor-suppressive effect of ZA-treated bone marrow.

Comparative cytokine analysis revealed that the ZA-resistant B2 cell line expressed higher levels of G-CSF, GM-CSF, CXCL1 and IL-18 than the ZA-responsive

B1 cell line (Supplemental Figure S3D). Various tumor-derived factors have been previously shown to induce osteoclastogenesis and osteoclast activity, including cell surface ligand Jagged1 and secreted factors RANKL, G-CSF, GM-CSF, MIP-1α, PTHrP, IL-8, IL-6, ICAM1 (30, 31). In particular, elevated plasma levels of G-CSF have been correlated with poor prognosis for patients with triple-negative breast cancer (32) and enhanced osteoclast activity has been reported in mice with elevated G-CSF levels (33-35). Although it is well established that G-CSF leads to increased numbers of myeloid cells in the bone marrow (35), whether G-CSF directly affects osteoclastogenesis or response to ZA is not well understood.

To assess whether G-CSF plays a role in resistance to ZA treatment that we had observed, we overexpressed G-CSF in the B1 cell line, which has endogenously low G-CSF expression, to generate a G-CSF-high cell line (B1-G) (Supplemental Figure S3E). Unlike the B1 bone metastases that were significantly reduced following ZA pre-treatment (~3-fold reduction; $p<0.05$), the B1-G metastatic burden was no different from that of the control cohort and significantly higher than that of B1 cells treated with ZA (Figure 3B-C). ZA also failed to suppress B1 metastases when G-CSF was administered systemically (Supplemental Figure S3F), even though the systemic efficacy of G-CSF was confirmed by an expected increase in peripheral neutrophil counts (Supplemental Figure S3G). Of note, neutrophil numbers in the bone marrow of B1 tumor-bearing mice was unchanged after ZA, G-CSF, or ZA+G-CSF administration (Supplemental Figure S3H) and G-CSF did not alter osteoclast activity relative to Ctl-treatment, as measured by plasma NTX (Supplemental Figure S3I).

To determine if G-CSF suppression is sufficient to confer ZA-response, we used two different shRNA constructs to suppress G-CSF in the B2 cell line, which has endogenously high G-CSF expression, to generate G-CSF-low cell lines (B2-shG1 and B2-shG2; Supplemental Figure S3E). At this time point, metastatic burden was not significantly affected following ZA pre-treatment regardless of G-CSF status in the B2 cells (Figure 3B-C, Supplemental Figure S3J). Likewise, neutralizing G-CSF *in vivo* prior to IC injection of the B2 cell line did not significantly reduce metastases following ZA pre-treatment (Figure 3D).

Together, these findings demonstrated that elevating G-CSF levels is sufficient to confer ZA resistance, but that suppression of G-CSF is not sufficient to induce ZA response. Moreover, these data indicated that G-CSF alone does not necessarily enhance metastatic burden above that of controls, but suggested that in the context of ZA treatment, G-CSF increases metastatic burden.

G-CSF prevents generation of tumor-suppressive M/OCPs

We next wondered if resistance to ZA under G-CSF-high conditions was due to counteracting effects of G-CSF on bone marrow hematopoietic cells. We started by analyzing the function of WBM harvested from C57BL/6 mice 5 days following administration of ZA, G-CSF, combination ZA+G-CSF, or vehicle control (Figure 4A).

As we observed repeatedly, WBM from ZA-treated mice inhibited B1 tumor formation *in vivo* (Figure 4B, Supplemental Figure S4A). We also confirmed that, as expected, ZA decreased osteoclast activity in these mice (Supplemental Figure S4B). While WBM from mice treated systemically with G-CSF did not significantly alter tumor

growth relative to that of the control cohort, when mice were treated systemically with combination ZA+G-CSF, their WBM was no longer tumor suppressive (Figure 4B, Supplemental Figure S4A). Importantly, both WBM and M/OCPs harvested from ZA-treated mice, which inhibited outgrowth of B1 tumor cells, were unable to inhibit growth of B1 tumor cells that overexpressed G-CSF (B1-G) (Figure 4C, Supplemental Figure S4C).

In concordance with our findings from the *in vitro* differentiation assays (Figure 2C-D), ZA significantly increased the numbers of macrophages in the marrow relative to vehicle control *in vivo* (Figure 4D). In contrast, WBM from mice treated systemically with G-CSF or with ZA+G-CSF contained similar numbers of macrophages as those of the Ctl cohort (Figure 4D).

These results suggested that G-CSF itself does not generate a marrow environment that enhances tumor growth relative to the control cohorts. Instead, G-CSF appeared to render ZA ineffective to generate tumor-suppressive marrow.

G-CSF counteracts ZA's ability to push differentiation of myeloid/osteoclast progenitors toward phagocytic macrophages

Our results thus far established that ZA alters the lineage potential of M/OCPs and renders them tumor-suppressive, while G-CSF mediates resistance to their tumor-suppressive effect. We therefore wished to know if G-CSF alters the lineage potential of the M/OCP population.

We first isolated WBM from Ctl-, ZA-, G-CSF, and ZA+G-CSF-treated mice and then treated the cells *in vitro* with M-CSF and RANKL (Figure 5A). As we repeatedly

observed, in the absence of G-CSF, WBM from the ZA-treated cohort gave rise to significantly fewer osteoclasts than those from the control cohorts (Figure 5B). However, WBM from G-CSF-treated animals gave rise to significantly more osteoclasts, even in the context of ZA treatment (Figure 5B).

We also isolated M/OCPs from Ctl- or ZA- treated mice and then treated the cells *in vitro* with M-CSF and RANKL in the presence or absence of G-CSF (Figure 5C). In the presence of G-CSF, M/OCPs from both Ctl- and ZA-treated mice gave rise to increased numbers of osteoclasts and decreased numbers of macrophages *in vitro* relative to M/OCPs in the absence of G-CSF (Figure 5D, 5E, Supplemental Figure S5A, S5B).

Our RNAseq analyses of M/OCPs from Ctl and ZA-treated mice (Fig. 1F) had suggested that ZA induces transcriptional changes consistent with monocyte/macrophage lineage bias. Therefore, to test potential functional consequences of altered M/OCP lineage potential, we added fluorescently labeled B1 tumor cells to the cultures resulting from M/OCP differentiation under various conditions, thus enabling us to assess macrophage phagocytic capacity by scoring their uptake of fluorescence. In the absence of G-CSF, macrophages derived from M/OCPs of ZA-treated mice had significantly enhanced phagocytic capacity relative to those from Ctl-treated mice, irrespective of adding RANKL to the culture (Figure 5F). In contrast, G-CSF significantly decreased the phagocytic capacity of the resulting culture from ZA-treated M/OCPs in both the undifferentiated (without RANKL) and differentiated (with RANKL) cultures (Figure 5F). Consistent with the phagocytic phenotype, numbers of F4/80 MHCII+ macrophages in the bone marrow of ZA-treated mice was ~3-fold higher

than in the control cohort, and G-CSF prevented this increase (Supplemental Figure S5C).

Collectively, these findings suggested that G-CSF counteracts the effect of ZA on M/OCP function and lineage potential at least in part by preventing ZA from inducing M/OCP differentiation toward phagocytic macrophages. Moreover, these results provide additional evidence to suggest an association between lineage potential and the tumor-inhibitory function of the bone marrow.

Bone marrow transcriptome and gene ontology processes that correlate with function

The results from our pre-clinical metastasis models thus far indicated that the status of the bone marrow at the time metastatic tumor cells encounter it has a profound influence on metastatic success. As such, we wanted to gain insights into how the whole bone marrow hematopoietic microenvironment is affected by ZA and how G-CSF may alter the ZA signature. We therefore characterized transcriptional programs (RNA-seq) on whole bone marrow from mice treated with Ctl, ZA, G-CSF, or combination ZA+G-CSF (GSE108250).

We first analyzed the RNA-seq data by identifying enriched gene ontology processes (36) within the lists of DEGs from each treatment condition (ZA, G-CSF, or ZA+G-CSF) as compared to Ctl-treated bone marrow (Supplemental Figure S6A-C, Supplemental Tables S3A-F). In the ZA-treated cohort, significantly enriched processes were related primarily to metabolic process whereas in the G-CSF-treated cohorts, as

well as in the ZA+G-CSF-treated cohorts, significantly enriched processes were dominated by immune processes (Supplemental Figure S6C).

A global analysis of gene expression differences between each of the 3 treatment cohorts (ZA, G-CSF, and ZA+G-CSF) and the control cohort (Ctl) provided insights into the effect of each treatment on WBM and M/OCPs. For WBM, the comparisons identified 56, 1,445 and 1,054 DEGs (modified BH adjusted p-value <0.01) in the ZA, G-CSF, and ZA+G-CSF cohorts, respectively (Figure 6A, Supplemental Figure S6A-B, Supplemental Table S4A-C). 779 DEGs were common to both the G-CSF and ZA+G-CSF comparisons, only 28 of which were also shared with the ZA comparison (Figure 6A). The 28 DEGs that were affected by all 3 treatments were the only DEGs shared between the ZA and ZA+G-CSF comparisons (Figure 6A). Importantly, 16 DEGs were affected exclusively by ZA treatment (i.e., not identified in the combined treatment comparison) and included genes involved in phagocytosis such as *Slc15a4, Usp37,* and *Ipo13* (Figure 6A and Supplemental Table S4A). Interestingly, ~25% of the DEGs resulting from combination ZA+G-CSF were unique to that treatment cohort (Figure 6A).

In the M/OCPs, 165 DEGs resulted from ZA treatment, 314 from G-CSF treatment, and 151 from combination ZA+G-CSF (Figure 6A, Supplemental Tables S5A, S5B, S5C). As observed with WBM, a number of DEGs (~38%) were unique to the combination treatment. 103 DEGs were affected exclusively by ZA treatment (Figure 6A). Interestingly, *Mapk8ip2* was one of the most significantly up-regulated DEGs in the ZA-treated cohort ($p=3.39x10^{-14}$), but was down-regulated in both G-CSF-treated ($p<8.48x10^{-4}$), and ZA+G-CSF-treated cohorts ($p=4.31x10^{-6}$). *Mapk8ip2* is involved in

monocyte differentiation into macrophages when activated (37) (Supplemental Table S5A).

These analyses revealed that both G-CSF and ZA significantly and uniquely affect transcriptional programs in the WBM and that combined treatment yields yet a different transcriptional profile from either treatment alone. Moreover, ZA treatment appeared to have a larger impact on M/OCPs than on WBM, while G-CSF appeared to dominate the effect on WBM.

Effects of ZA that are lost or significantly changed in the presence of G-CSF

We considered the transcriptional effects we observed with each treatment and the fact that ZA treatment generated metastasis-suppressive marrow while G-CSF alone had no effect on metastatic burden, yet G-CSF induced resistance to ZA and increased metastatic burden in the context of ZA treatment. In doing so, we speculated that ZA and G-CSF either affect the marrow in opposing directions or that the effects of combination treatment cannot be explained by contributions of either treatment alone.

Our comparative analysis revealed that the DEGs upon combination treatment were not equivalently significant in either the ZA or G-CSF cohorts (Figure 6A). In other words, none of these genes was expressed in an opposing manner. Indeed, 263 DEGs were unique to WBM and 58 genes unique to the M/OCP population in the ZA+G-CSF cohorts (Figure 6A). Hence, we employed a regression approach with an interaction term and identified genes for which the effects of G-CSF and ZA statistically interact (Figure 6B, Supplemental Table S6A-B).

GO analysis of these non-additively differentially expressed genes from WBM revealed processes significantly enriched by the combination treatment that described the difference in response to ZA in the presence of G-CSF (Figure 6C, Supplemental Table S7). The enrichment list represents gene sets that were either enhanced or ablated relative to the cumulative effects expected from adding together the effects of ZA and G-CSF treatments alone, including those newly emerging with combination treatment. Of these, “immune response” and “phagocytosis” were particularly intriguing to us, as these were predominantly suppressed by combination treatment. For example, a number of genes involved in antigen processing and lymphocyte activation, including *B2m, Vav2*, and a number of histocompatibility genes (*H2-K1, H2-D1, H2-Q5, H2-Q7*) were uniquely suppressed with ZA+G-CSF combination treatment relative to Ctl treatment (Supplemental Table S6A). Moreover, *Axl*, which suppresses myeloid cell immune function and dampens NK cell activity (38), was significantly suppressed by ZA treatment (log2(Fold Change)= -1.20, $p=1.25x10^{-4}$) but significantly enhanced with ZA+G-CSF treatment (log2(Fold Change)=1.68, $p=2.7x10^{-5}$) (Supplemental Table S6A)

Together with our pre-clinical modeling, these analyses indicated that in the marrow of animals treated with combination ZA + G-CSF, the transcriptional effects of ZA are negated and/or significantly changed by G-CSF in a manner that associates with metastatic progression.

High plasma G-CSF correlates with worse outcome for breast cancer patients treated with adjuvant ZA

Our pre-clinical data established that G-CSF mediates resistance to ZA, and in fact, ZA+G-CSF combination treatment had unexpected effects on the metastatic microenvironment, resulting in enhanced metastasis relative to ZA treatment alone. Hence, we sought to understand if patient plasma G-CSF levels correlate with response to ZA. In the clinical setting, bisphosphonates have suggested benefit, as demonstrated by results from a meta-analysis in which patients who had received adjuvant bisphosphonate treatment observed a significant reduction in breast cancer recurrence in the bone (39). Nevertheless, responses have been limited for unknown reasons and biomarkers that can be used to guide treatment decisions are lacking.

We analyzed patient plasma samples (n=392) from the AZURE clinical trial in which women with stage II/III breast cancer were randomized to receive standard systemic treatment (>95% of the patients received chemotherapy) with or without adjuvant ZA (16) (Figure 7A). In the AZURE trial, postmenopausal (natural or induced with ovarian suppression) patients observed a significant decrease in overall breast cancer recurrence (16). Importantly, primary G-CSF prophylaxis was not used in these patients. We verified that the magnitude of effect of ZA in reducing the development of bone metastasis at any time during the 10-year follow-up in our patient subset was similar to that of the overall trial (trial total n=3,360, hazard ratio (HR)=0.81, 95% confidence interval (CI) 0.68-0.97 (16); our subset n=392, HR=0.89, 95% CI 0.62-1.3) (Figure 7A).

We utilized an analytical approach that adjusts for an optimal plasma G-CSF concentration cut point and enables us to accurately determine DFS and significance levels in an unbiased fashion (40) (See Methods, Supplemental Figure 7A-D). Based on

these previously published methods, we determined that a plasma G-CSF concentration of 23 pg/mL was the optimum cut-point for assessing disease-free survival (DFS) events in ZA-treated patients (40).

Patients receiving adjuvant ZA whose plasma G-CSF levels were > 23 pg/mL at the time of randomization had significantly reduced DFS when compared with patients with plasma G-CSF levels < 23 pg/mL (p adjusted=0.02) as assessed over a 10-year period (Figure 7B). However, in the cohort that did not receive ZA, plasma G-CSF levels did not predict a significant difference in DFS (Supplemental Figure S7B). Cox model analysis demonstrated that the relationship between high plasma G-CSF levels and DFS in ZA-treated patients could not be explained by imbalances in other key prognostic variables, namely number of involved lymph nodes affected, tumor size (T stage), and breast cancer receptor status (ER/PR/Her2). Moreover, in support of the retrospective analyses demonstrating that post-menopausal patients observed significant benefit with adjuvant ZA, plasma G-CSF levels were significantly lower in post-menopausal patients than pre-menopausal patients in our cohort ($p=1.14x10^{-4}$).

DISCUSSION

This work revealed that bone marrow hematopoietic cell states, particularly M/OCP lineage potential, have a profound impact on breast cancer bone metastasis and that the hematopoietic microenvironment, which serves as a niche for disseminated tumor cells, can be modulated by bone-targeting agents and cytokines to alter disease outcome. Specifically, the bisphosphonate, ZA, directs M/OCP lineage potential toward tumor-suppressive macrophages and prevents metastatic growth in the bone; systemic

or tumor-derived G-CSF promotes resistance to the metastasis-suppressive effect of ZA by skewing M/OCP differentiation toward osteoclasts and away from the phagocytic myeloid lineage (Figure 7C).

Further mechanistic investigation into the newly identified biology that we report here is warranted in order to understand how best to capitalize on bone marrow and M/OCP function and differentiation potential to prevent or limit metastatic disease in the bone. The novel, perhaps unexpected effect of ZA on the bone microenvironment may provide one such avenue. From a clinical perspective, targeting osteoclast activity with bone-modifying agents, such as bisphosphonates or the RANK-ligand inhibitor denosumab, has significantly reduced skeletal-related events patients with metastatic breast cancer to the bone (i.e. bone fractures, bone pain requiring radiation therapy, spinal cord compression, and hypercalcemia), (41). Thus, current NCCN guidelines support the administration of these agents in combination with chemotherapy or endocrine therapy for patients with bone metastases (category 1 recommendation) (42, 43). Results from a meta-analysis of individual patient data from 18,766 women – enrolled over 26 randomized trials that evaluated the benefits of adjuvant bisphosphonate treatment – showed a significant reduction in bone recurrence and improvement in breast cancer specific survival (44).

Subgroup analyses have suggested that postmenopausal status, but not hormone receptor (ER/PR) or growth factor receptor (Her2) expression, predisposes patients who are more likely to benefit from bisphosphonates, and this is reflected in the recently published guidelines by Cancer Care Ontario (CCO) and the American Society of Clinical Oncology (ASCO) that recommend consideration of zoledronic acid (ZA) or

clodronate for postmenopausal (natural or induced with ovarian suppression) patients deemed candidates for adjuvant systemic therapy (43). Other meta-analyses revealed that adjuvant therapy with ZA increases overall survival in early stage breast cancer (44). Additionally, ZA decreased the number of DTCs in the bone marrow of Stage II/III breast cancer patients in a randomized clinical trial (45). ZA has also been demonstrated to increase disease free survival when it is administered with neoadjuvant chemotherapy, particularly in post-menopausal patients (46). Nevertheless, an underlying biological explanation for the protective effect of bisphosphonates in breast cancer, in terms of reduction of disease recurrence, had remained elusive.

Although meta-analyses of the clinical studies highlighted efficacy of ZA, no overall survival benefit has been reported to date in individual randomized controlled trials in breast cancer. Consequently, even considering pre- or post-menopausal status, it remained unclear how to identify which patients would observe benefit with ZA (16). Our findings provide new insights into why certain patients may not see reduction in breast cancer recurrence with ZA. Our pre-clinical findings are underscored by the fact that patients in the AZURE trial (16) with higher plasma G-CSF levels experienced worse outcome from adjuvant ZA-treatment and provide preliminary evidence to caution against the use of ZA in patients with high plasma G-CSF. High plasma G-CSF, however, has been correlated with poor prognosis in breast cancer patients, specifically those with triple-negative breast cancer (32). However, in our study, plasma G-CSF levels alone, in the absence of ZA treatment, did not predict worse survival.

Unfortunately, our findings provide a preliminary indication that suppression of G-CSF may not be an effective strategy for improving responses to ZA, as neither genetic

nor pharmacological inhibition of G-CSF was sufficient to confer response. It is possible that the balance between tumor-promoting (8) and tumor-suppressive cells in the marrow, or other cytokines (such as GM-CSF) must be considered in the appropriate contexts. Further studies to evaluate our findings will therefore require well-designed pre-clinical and clinical trials to determine patient benefit with adjuvant ZA in the presence or absence of G-CSF administration. Our analyses suggest other ways to achieve this goal may be to include combinations with other bone-targeting agents or immunotherapies. Further studies based on results of our gene expression profiling under these various conditions may reveal factors, pathways, and processes that are necessary and/or sufficient for the tumor inhibitory function of the bone marrow. Some of the newly identified gene products presented here may be considered as candidate targets for future combination therapies and pre-clinical research.

Likewise, additional work will be necessary to determine the translatability of G-CSF as a biomarker for selection of patients who should/should not receive ZA treatment, given that many patients also receive G-CSF at the time of chemotherapy and adjuvant ZA treatment (the patients in our study did not receive primary G-CSF prophylaxis and less than 10% received secondary G-CSF treatment). Identifying biomarkers that better stratify patient risk and responses to ZA hold the potential of using bone-modulating drugs to improve patient outcomes.

Identification of a tumor-suppressive population in the bone marrow provides opportunities for exploring new therapeutic strategies that could generate such cells in order to halt metastatic progression or overcome the adverse effects of G-CSF. The ability to use relatively safe bone-modulating therapeutics to capitalize on the tumor-

suppressive function of the bone marrow, particularly M/OCP populations, provides a foundation for potentially curative treatments during the time when metastatic breast cancer can still be controlled.

ACKNOWLEDGEMENTS

This work was supported by funds from NIH T32 GM007226 and NCI F31CA195797 (J. Ubellacker); NIH R01DK107784 and U54CA163191 (D. Scadden); DOD Era of Hope W81XWH-14-1-0191 and NIH NCI RO1 CA166284 Presidential Early Career Award for Scientists and Engineers (S. McAllister). We are grateful to the patients who participated in the AZURE trial. We thank P. Ottewell and G. van der Plujm for generous donation of MDA-MB-231 bone-tropic cell lines; J. Brown, H. Shulver, and J. Horsman for assistance with obtaining clinical trial samples; and the Boston Children's Hospital Heme/Onc-HSCI Flow Cytometry facility (Boston, MA, USA). We thank members of the McAllister and Scadden laboratories and Drs. Bruce Zetter, Karen Cichowski and Nancy Lin for helpful discussion; L. Rooney, J. Olive, Z. Castano for technical review of the manuscript; J. Ferlic for biostatistics assistance; R. Tadipatri for technical assistance; A. Molineaux and M. Petit for administrative assistance. We are also grateful to N. Tung and J. Garber for helpful discussion in early stages of the project.

REFERENCES

1. Colleoni M, Sun Z., Price K.N., Karlsson P., Forbes J.F., Thurlimann B., *et al.* (2016). Annual hazard rates of recurrence for breast cancer during 24 years of follow-up: results

from the International Breast Cancer Study Group trials I to V. *J Clin Oncol.* 34(9), 927-935.

2. Press DJ, Miller ME, Liederbach E, *et al.* (2017). De novo metastasis in breast cancer: occurrence and overall survival stratified by molecular subtype. *Clin Ex Metastasis.* ISSN: 1573-7276.

3. Gnant M. and Hadji P. (2010). Prevention of bone metastases and management of bone health in early breast cancer. *Breast Cancer Res.* 12(6), 216.

4. Tjensvoll K, Oltedal S, Heikkila R. (2012). Persistent tumor cells in bone marrow of non-metastatic breast cancer patients after primary surgery are associated with inferior outcome. *BMC Cancer.* 12(190).

5. Ren G., Esposito M., Kang Y. (2015). Bone metastasis and the metastatic niche. *J. Mol. Med.* 93(11):1203–1212.

6. Guise T. (2010). Examining the metastatic niche: targeting the microenvironment. *Semin. Oncol.* 37(Suppl. 2):S2–S14.

7. Rack, B., Junckstock J., Gunthner-Biller M., Andergassen U., Neugebauer J., Hepp P., *et al.* (2011). Trastuzumab Clears HER2/neu-positive isolated tumor cells from bone marrow in primary breast cancer patients. *Arch Gynecol Obstet* 285(2), 485-492.

8. McAllister S.S., Weinberg R.A. (2014). The tumour-induced systemic environment as a critical regulator of cancer progression and metastasis. *Nat. Cell Biol.* 16(8):717–727.

9. Engblom C, Pfirschke C, Pittet MJ. (2016). The role of myeloid cells in cancer therapies. *Nature Rev Cancer.* 16(7), 447-62.

10. Gao, D., Mittal, V. (2009). The role of bone-marrow-derived cells in tumor growth, metastasis initiation and progression. *Trends Mol Med*. 15(8):333-43.

11. Morrison, S.J. and Scadden D.T. (2014). The bone marrow niche for haematopoietic stem cells. *Nature.* 505(7483), 327–34.

12. Kollet O, Dar A., Shivtiel S., Kalinkovich A., Lapid K., Sztainberg Y., *et al.* (2006). Osteoclasts degrade endosteal components and promote mobilization of hematopoietic progenitor cells. *Nature Medicine*. June 12(6), 657-64.

13. Nilsson SK, Johnston HM, Whitty GA, Williams B, Webb RJ, Denhardt DT, *et al.* (2005). Osteopontin, a key component of the hematopoietic stem cell niche and regulator of primitive hematopoietic progenitor cells. *Blood*. 106(4), 1232-9.

14. Stier S, Ko Y, Forkert R, Lutz C, Neuhaus T, Grunewald E, *et al.* (2005). Osteopontin is a hematopoietic stem cell niche component that negatively regulates stem cell pool size. *J Exp Med.* 201(11):1781-91.

15. Ubellacker J.M., Haider M.T., DeCristo M.J., Allocca G., Brown N.J., Silver D.P., *et al.* (2017). Zoledronic acid alters hematopoiesis and generates breast tumor-suppressive bone marrow cells. *Breast Cancer Res.* 19: 23.

16. Coleman R., Cameron D., Dodwell D., Bell R., Wilson C., Rathbone E., *et al.* (2014). Adjuvant zoledronic acid in patients with early breast cancer: final efficacy analysis of the AZURE (BIG 01/04) randomised open-label phase 3 trial. *Lancet Oncol.* 15, 997-1006.

17. Marsh T., Wong I., Sceneay J, Barakat A, Qin Y, Sjodin A, Alspach E, Nilsson B, Steward SA, McAllister SS (2016). *Cancer Res.* 15;76(10):2932-43.

18. McAllister S.S., Gifford A.M., Greiner A.L., Kelleher S.P., Saelzler M.P., Ince T.A., *et al.* (2008). Systemic endocrine instigation of indolent tumor growth requires osteopontin. *Cell.* 133, 994-1005.

19. Boyle W.J., Simonet W.S., Lacey D.L. (2003). Osteoclast differentiation and activation. *Nature.* 423, 337–342.

20. Jacome-Galarza C.E., Lee S.K., Lorenzo J.A., Aguila J.A. (2013). Identification, characterization and isolation of common progenitor for osteoclasts, macrophages, and dendritic cells from murine bone marrow and periphery. *J Bone Miner Res.* 28(5),1203

21. Miyamoto, T. (2013). Identification and characterization of osteoclast precursor cells. *BoneKEy* 346.

22. Zhu, L., Zhao, Q., Yang, T., Ding, W. & Zhao, Y. (2015). Cellular metabolism and macrophage functional polarization. *Int. Rev. Immunol.* 34, 82-100.

23. Martinez, F., Gordon, S., Locati, M., Mantovani, A. (2006). Transcriptional profiling of the human monocyte-to-macrophage differentiation and polarization: new molecules and patterns of expression. *J Immunol.* 177(10) 7303-7311.

24. Hirbe A.C., Roelofs A.J., Floyd D.H., Deng H., Becker S.N., Lanigan L.G., *et al.* (2009). The bisphosphonate zoledronic acid decreases tumor growth in bone in mice with defective osteoclasts. *Bone*. 44(5):908-916.

25. Zhang K., Kim S., Cremasco V., Hirbe A.C., Novack D.V., Weilbaecher K., *et al.* (2011). CD8+ T cells regulate bone tumor burden independent of osteoclast resorption. *Cancer Res.* 15;71(14):4799-808.

26. Dougall W.C., Glaccum M., Charrier K., Rohrbach K., Brasel K., De Smedt T., *et al.* (1999). RANK is essential for osteoclast and lymph node development. *Genes Dev.* 13, 2412-24.

27. Ari F., Miyamoto T., Ohneda O., Inada T., Sudo T., Brasel K., *et al.* (1999). Commitment and differentiation of osteoclast precursor cells by the sequential expression of c-fms and RANK receptors. *J. Exp. Med.* 190(12), 1741-1754.

28. Wetterwald A., van der Pluijm G., Que I., Sijmons B., Buijs J., Kaperien M., *et al.* (2002). Optical imaging of cancer metastasis to bone: a mouse model of minimal residual disease. *Am J Pathol.* 160(3), 1143-1153.

29. Nutter F., Holen I., Brown H.K., Cross S.S., Evans C.A., Walker M., *et al.* (2014). Different molecular profiles are associated with breast cancer cell homing compared to colonisation of bone—evidence using a novel bone-seeking cell line. *Endocrine-related cancer*. 21(2), 327-41.

30. Ell B. and Kang Y. (2012). Bone Metastasis. *Cell.* 26;151(3), 690.

31. Weilbaecher K.N., Guise T.A., McCauley L.K. (2011). Cancer to bone: a fatal attraction. *Nat Rev Cancer.* 11(6), 411-425.

32. Hollmén M., Karaman S., Schwager S., Lisibach A., Christiansen A.J., Maksimow M, *et al.* (2015). G-CSF regulates macrophage phenotype and associates with poor overall survival in human triple-negative breast cancer. *Oncoimmunology.* 24;5(3), e1115177.

33. Takahashi T., Wada T., Mori M., Kokai Y., Ishii S. (1996). Overexpression of the granulocyte colony-stimulating factor gene leads to osteoporosis in mice. *Lab Invest.* 74, 827-834.

34. Hirbe A.C., Uluckan O., Morgan E.A., Eagleton M.C., Prior J.L., Piwnica-Worms D., *et al.* (2007). Granulocyte colony-stimulating factor enhances bone tumor growth in mice in an osteoclast-dependent manner. *Blood.* 109, 3424-3431.

35. Christopher M.J., Link. D. C. (2008). Granulocyte colony-stimulating factor induces osteoblasts apoptosis and inhibits osteoblast differentiation. *J Bone and Miner Res.* 23(11), 1765-1774.

36. Reimand, J., Kull, M., Peterson, H., Hansen, J., & Vilo, J. (2007). G:Profiler-a web-based toolset for functional profiling of gene lists from large-scale experiments. *Nucleic Acids Research*, 35(SUPPL.2), W193–W200.

37. Hale, K.K., Trollinger, D., Rihanek, M., Manthey, C.L. (1999). Differential expression and activation of p38 mitogen-activated protein kinase α, β, γ and δ in inflammatory cell lineage. *J. Immunology*. 162, 4246-4252.

38. Ludwig K.F., Du W., Sorrelle N.B., Wnuk-Lipinska K., Topalovski M., Toombs J.E., *et al.* (2017). Small molecule inhibition of Axl targets tumor immune suppression and enhances chemotherapy in pancreatic cancer. *AACR Journals OnlineFirst*.

39. Early Breast Cancer Trialists' Collaborative Group (EBCTCG). (2015). Adjuvant bisphosphonate treatment in early breast cancer: meta-analyses of individual patient data from randomised trials. *Lancet.* 386(10001), 1353-1361.

40. Viprey V.F., Gregory V.M., Corrias M.V., Tchirkov A., Swerts K., Vicha A., *et al.* (2014). Neuroblastoma mRNAs Predict Outcome in Children with Stage 4 Neuroblastoma: A European HR-NBL1/SIOPEN Study. *J Clin Oncol.* 1;32(10), 1074-83.

41. Stopeck A.T., Lipton A., Body J.J., Steger G.G., Tonkin K., de Boer R.H, *et al.* (2010). Denosumab compared with zoledronic acid for the treatment of bone metastases in patients with advanced breast cancer: A randomized, double-blind study. *Journal of Clinical Oncology.* 28(35).

42. Gradishar W.J., Anderson B.O., Balassanian R., Blair S.L., Burstein H.J., Cyr A., *et al.* (2017). Breast Cancer, Version 1.2017. NNCN Guidelines Insights. *J of Nat Compr Canc Netw.* 15(4).

43. Dhesy-Thind S., Fletcher G.G., Blanchette P.S., Clemons M.J., Dillmon M.S., Frank E.S., *et al.* (2017). Use of Adjuvant Bisphosphonates and Other Bone-Modifying Agents in Breast Cancer: A Cancer Care Ontario and American Society of Clinical Oncology Clinical Practice Guideline. *J. of Clin. Oncol.* 35(18), 2062-2080.

44. Valachis A, Polyzos NP, Coleman RE, Gnant M, Eidtmann H, Brufsky AM, *et al.* (2013). Adjuvant therapy with zoledronic acid in patients with breast cancer: a systemic review and meta-analysis. *Oncologist*. 18(4):353-61.

45. Aft R.L., Naughton M., Trinkaus K., Watson M, Ylagan L., Chavez-MacGregor, *et al.* (2010). Effect of zoledronic acid on disseminated tumour cells in women with locally advanced breast cancer: an open label, randomized, phase 2 trial. *The Lancet Oncology*. 11(5):421-428.

46. Kroep J.R., Charehbili A., Coleman R.E., Aft R.L., Hasegawa Y., Winter M.C., *et al.* (2016). Effects of neoadjuvant chemotherapy with or without zoledronic acid on pathological response: A meta-analysis of randomized trials. *Eur J Cancer*. 54: 57-63.

FIGURE LEGENDS

Figure 1. Identification of therapeutically induced tumor-inhibitory hematopoietic bone marrow cells

(**A**) Experimental scheme for assay to test bone marrow cell (BMC) tumor support function. Whole bone marrow (WBM) or various FACS-isolated bone marrow populations were harvested from zoledronic acid (ZA)- or vehicle-treated control (Ctl) donor mice at either 5 days (C57BL/6) or 3 days (Nude) and mixed with tumor cells immediately prior to injection into recipient mice and tumor incidence and growth kinetics measured over time.

(**B**) Incidence (%) of subcutaneous tumor formation in nude recipient mice at experimental endpoint (d14) resulting from $2.5x10^5$ MDA-MB-231-B1 (B1) cells admixed with matrigel (NA, no donor BMCs included) or $7.5x10^5$ WBM cells from Ctl or ZA treated nude and C57BL/6 donors (n=4-7 injections per cohort, statistics representative of 2 biological replications).

(**C**) Incidence (%) of subcutaneous tumor formation in nude recipient mice at experimental endpoint (d14) resulting from $2.5x10^5$ MDA-MB-231-B1 (B1) cells admixed with $7.5x10^5$ whole BMCs (WBM), $7.5x10^5$ Lin+ BMCs, or $2.5x10^5$ Lin- BMCs from Ctl or ZA treated nude donors. Data for each ZA-treated cohort are represented relative to its respective Ctl-treated cohort; (n=20-24 injections per cohort). Lin- populations were sorted by gating on: CD3- Ly-6G/Ly6-C- Cd11b- CD45R- and TER119- and all of the remaining BMCs were used as the Lin+ populations.

(**D**) Number of myeloid/osteoclast progenitor cells (M/OCPs; Lin-CD115+) in bone marrow of C57BL/6 mice at indicated time points after ZA treatment (n=4-5 mice per cohort, representative of 3 biological replications).

(**E**) Incidence (%) of tumor formation in nude recipient mice at experimental endpoint (d14) resulting from $2.5x10^5$ B1 cells admixed with $7.5x10^5$ WBM cells, 10^5 sorted M/OCPs, or $6.5x10^5$ M/OCP-depleted BMCs from Ctl- or ZA-treated C57BL/6 donors (n=6 injections per cohort, statistics representative of 2 biological replications). Controls from different cohorts are not compared due to the fact that different numbers of BMCs are admixed with tumor cells in each case.

(**F**) GSEA analysis (clusterProfiler tool using KEGG gene sets) and gprofileR (GO) analysis of the differentially expressed genes in M/OCPs isolated from ZA-treated mice

as compared to M/OCPs isolated from Ctl-treated mice. Significance was determined as described in Methods: RNA-sequencing.

Error bars represent mean ± SEM; two-tailed t-tests (unpaired) were used to determine statistical significance, *p<0.05, ***p<0.001.

Figure 2. ZA skews lineage potential of myeloid/osteoclast progenitor cells toward macrophages

(**A**) Experimental scheme for *in vitro* osteoclast (OC) differentiation assay with whole bone marrow (WBM) or M/OCPs from Ctl- or ZA-treated C57BL/6 donors.

(**B**) Quantification of OCs (TRAP+, multinucleated cells) at endpoint of *in vitro* OC differentiation assay (d5) with WBM from Ctl- or ZA-treated C57BL/6 donors (n=5 donor samples/cohort; representative of 3 biological replications).

(**C-D**) Flow cytometric quantification of macrophages (Mϕs); Cd11b+/F4/80+/MHCII+) and dendritic cells (DCs; Cd11b+/MHCII+/Cd11c+) from sorted WBM populations (C) (n=5 donor samples/cohort; representative of 3 biological replications) or M/OCPs (D) (n=6-7 donor samples/cohort; representative of 3 biological replications) from Ctl- or ZA-treated C57BL/6 donors at endpoint (d5) of OC differentiation assay. Error bars represent mean ± SEM; two-tailed t-tests (unpaired) were used to determine statistical significance, *p<0.05.

Figure 3. ZA inhibits breast cancer metastasis in a manner that is counteracted by G-CSF

(**A**) Experimental scheme for intracardiac (IC) injections of indicated breast tumor cells

into Ctl or ZA pre-treated nude mice.

(**B**) Total tumor burden at experimental end point as quantified by bioluminescence imaging (n=4-9/cohort); representative of 3 biological repetitions.

(**C**) Representative bioluminescence images from indicated cohorts in (B) at experimental end point.

(**D**) Experimental scheme for IC injections of B2 cell line following pre-treatment with Ctl or ZA and a G-CSF neutralizing antibody or isotype-matched control antibody (IMC) (top). Graph represents total tumor burden at experimental end point (d10) as quantified by bioluminescence imaging of the luciferase+ B2 cell line. All mice had signal present. (d10) (n=4-5/cohort).

Throughout, error bars represent mean ± SEM; two-tailed t-tests (unpaired) were used to determine statistical significance, *$p<0.05$.

Figure 4. G-CSF prevents generation of tumor-suppressive M/OCPs

(A) Experimental scheme for assay to test tumor support function of BMCs from indicated donor mice.

(B) Incidence (%) of subcutaneous tumor formation in nude recipient mice at experimental end point (d14) resulting from B1 cells admixed with WBM from Ctl-, ZA-, G-CSF (G)-, or ZA+G-CSF (ZA+G)-treated C57BL/6 donors (n=4-6 tumors per cohort, statistics representative of 2 biological replications).

(C) Incidence (%) of tumor formation in nude recipient mice at experimental end point (d14) resulting from B1 or B1-G cells admixed with WBM or sorted M/OCPs from Ctl- or

ZA- treated C57BL/6 donors (n=4-6 tumors per cohort, statistics representative of 2 biological replications).

(D) Quantitative flow cytometric analysis of WBM from indicated mice for number of macrophages (Cd11b+/F4/80+/MHCII+) 3 days after Ctl (C), ZA (Z), G-CSF (G), or G-CSF+ZA (G+Z) treatment (n=4-5/cohort; representative of 3 biological replications).

Throughout, error bars represent mean ± SEM; two-tailed t-tests (unpaired) were used to determine statistical significance, *p<0.05.

Figure 5. G-CSF counteracts ZA's ability to push differentiation of myeloid/osteoclast progenitors toward phagocytic macrophages

(**A**) Experimental scheme for *in vitro* osteoclast differentiation assay using bone marrow from Ctl-, ZA-, G-CSF- or ZA+G-CSF-treated C57BL/6 donors

(**B**) Quantification of osteoclasts (OC, TRAP+, multinucleated cells) at endpoint (d5) of *in vitro* osteoclast differentiation assay with 1,000 WBM per well Ctl, ZA, G-CSF or ZA+G-CSF treated C57BL/6 donors (n=4 donor samples/cohort; representative of 3 biological replications).

(**C**) Experimental scheme for *in vitro* osteoclast differentiation assay using bone marrow from Ctl- or ZA-treated C57BL/6 donors that were subsequently treated with Ctl or recombinant hG-CSF *in vitro* at d3

(**D**) Quantification of osteoclasts (OC, TRAP+, multinucleated cells) at endpoint (d5) of *in vitro* osteoclast differentiation assay with 250 M/OCPs per well from Ctl or ZA treated C57BL/6 donor mice; M/OCPs were treated *in vitro* with RANKL ± G-CSF (n=4 donor samples per cohort; representative of 3 biological replications).

(**E**) Flow cytometric quantification of macrophages (Cd11b+/F4/80 MHCII+) at end point of *in vitro* OC differentiation assay (d5) using sorted M/OCPs from Ctl or ZA treated C57BL/6 mice; M/OCPs were subsequently treated *in vitro* with M-CSF and RANKL ± G-CSF (n=4 donor samples per cohort; representative of 3 biological replications).
(**F**) Percent of phycoerythrin (PE)-positive M/OCP-derived macrophages (Cd11b+ F4/80+ MHCII+) at end point (d5), indicating phagocytosis of Did-Cm (PE)-labeled B1 tumor cells (n=4 donor samples per cohort, representative of 3 biological replications). Error bars represent mean ± SEM; two-tailed t-tests (unpaired) were used to determine statistical significance, *p<0.05, **p<0.01.

Figure 6. Bone marrow transcriptome and gene ontology processes that correlate with function

(A) Venn-Diagrams for distinct and non-distinct differentially expressed genes in the bone marrow (left) or M/OCPs (right) from mice treated with ZA (blue), G-CSF (red) or ZA+G-CSF ("Both", yellow), as normalized to Ctl-treated bone marrow or M/OCPs (modified BH adjusted p-value less than 0.01).
(B) Heatmap of expression levels of genes identified from a regression analysis of the interaction between G-CSF and ZA effects on gene expression for whole bone marrow (left) or M/OCPs (right). Individual sample expression levels are shown for genes with a modified BH adjusted p-value of less than 0.01 from the regression. Values represent normalized counts after centering on the mean expression levels of the control samples and scaling to the range of gene expression across all samples (so that -1 represents the lowest expression level for all samples and 1 the highest).

(C) Enriched gene ontology categories for genes for which the simultaneous effects of G-CSF and ZA treatment on expression were not additive in a comparative analysis model for whole bone marrow. Categories for each indicated cohort were compared to control using the non-additive genes (as ordered by absolute log2 fold change; modified BH adjusted p-value less than 0.01 A list of the statistically enriched gene ontology (GO) terms for biological processes was generated using the methods described in (A)).

Figure 7. High plasma G-CSF correlates with worse outcome for breast cancer patients treated with adjuvant ZA

(**A**) AZURE clinical trial randomization scheme from Coleman et al., 2014 (16) and Cox proportional hazards model analysis of subgroup from AZURE trial (n=392) for DFS by Ctl and ZA cohorts, menopausal status, and by menopausal status for treatment group; *p<0.05.

(**B**) Disease-free survival (DFS) outcome (derived from cut point analysis—see STAR methods) defined in terms of number of DFS events avoided/saved over the 10-year period post randomization among ZA-treated patients; optimal cut point was at 23 pg/mL G-CSF.

(C) Proposed model. ZA inhibits mature osteoclasts and also increases the numbers of M/OCPs in the BM, altering their gene expression profile to drive them toward tumor suppressive phagocytic macrophages. Tumor-derived or systemic G-CSF counteracts the effects of ZA by driving the lineage potential of M/OCPs toward osteoclasts.

Figure 1

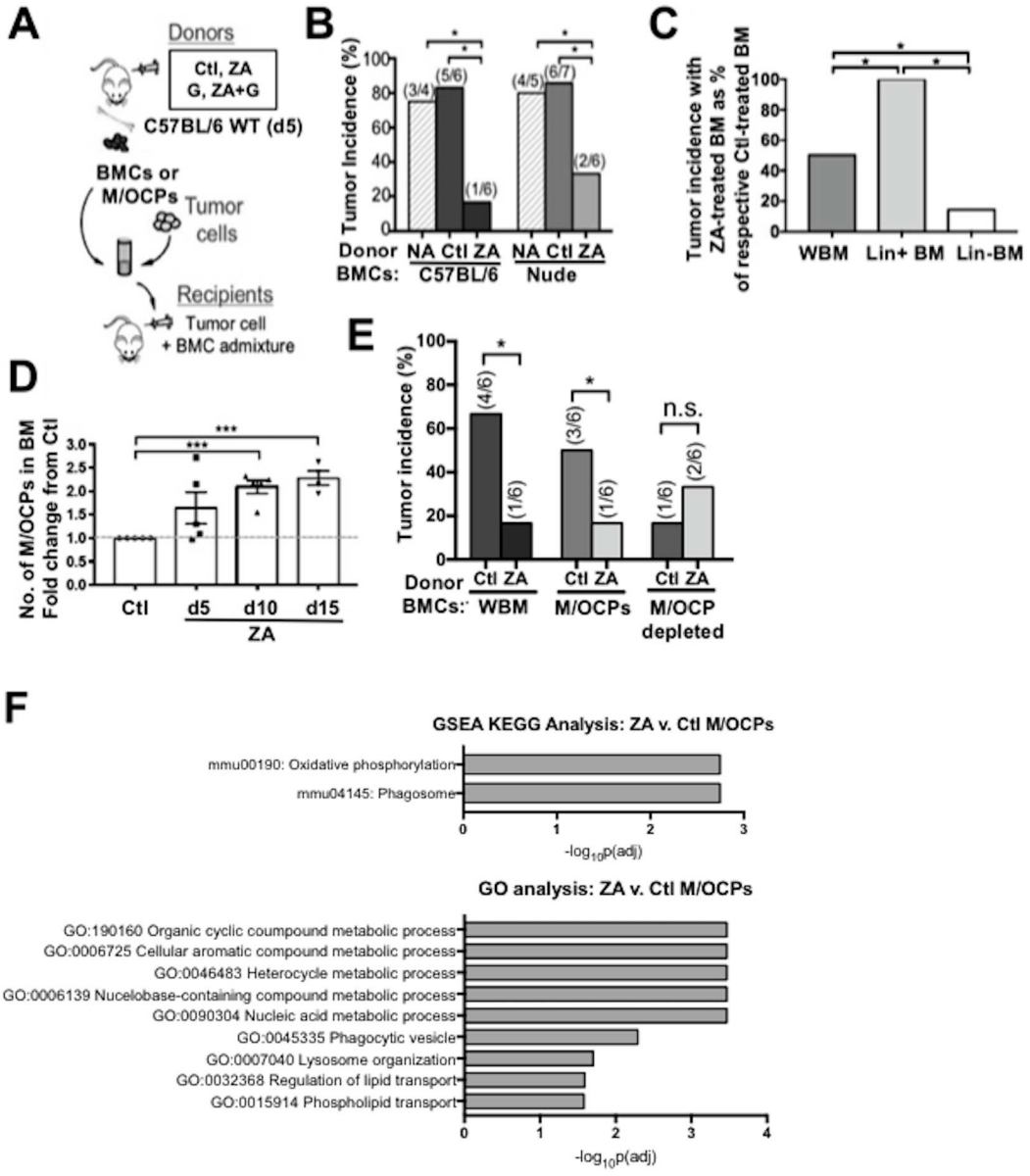

Figure 2

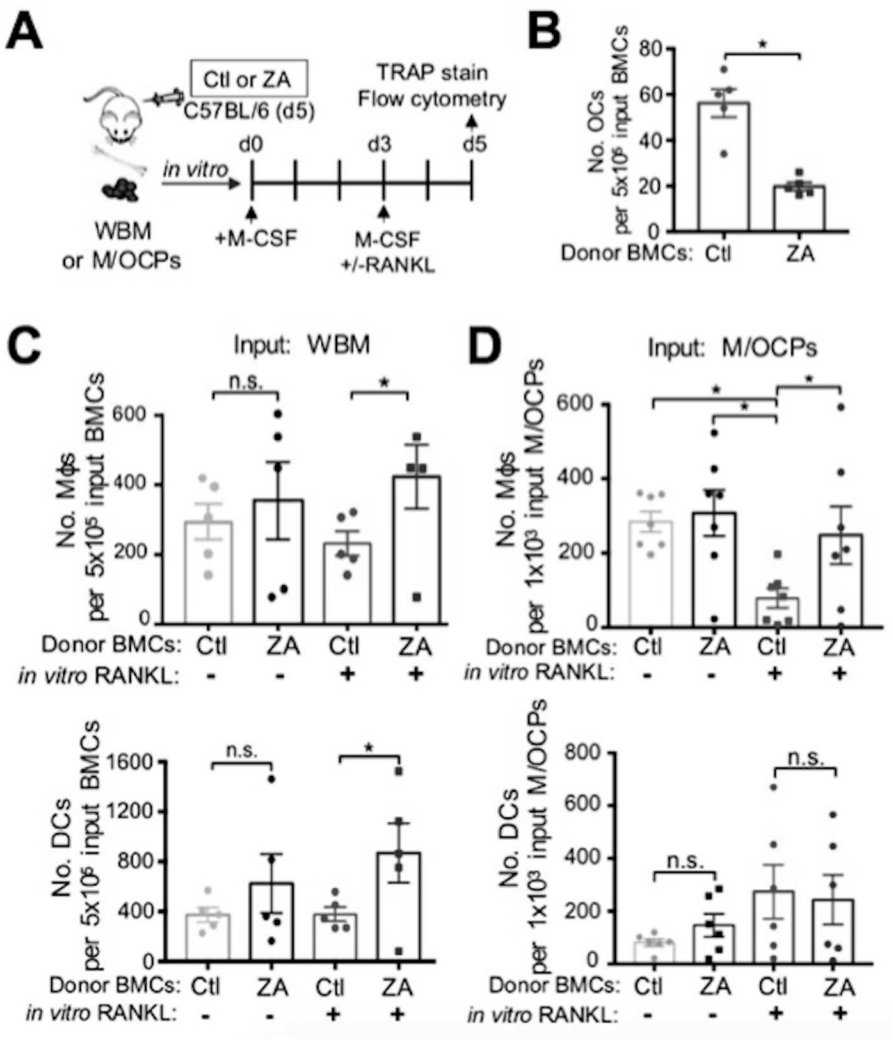

Author Manuscript Published OnlineFirst on July 31, 2018; DOI: 10.1158/0008-5472.CAN-18-0548
Author manuscripts have been peer reviewed and accepted for publication but have not yet been edited.

Figure 3

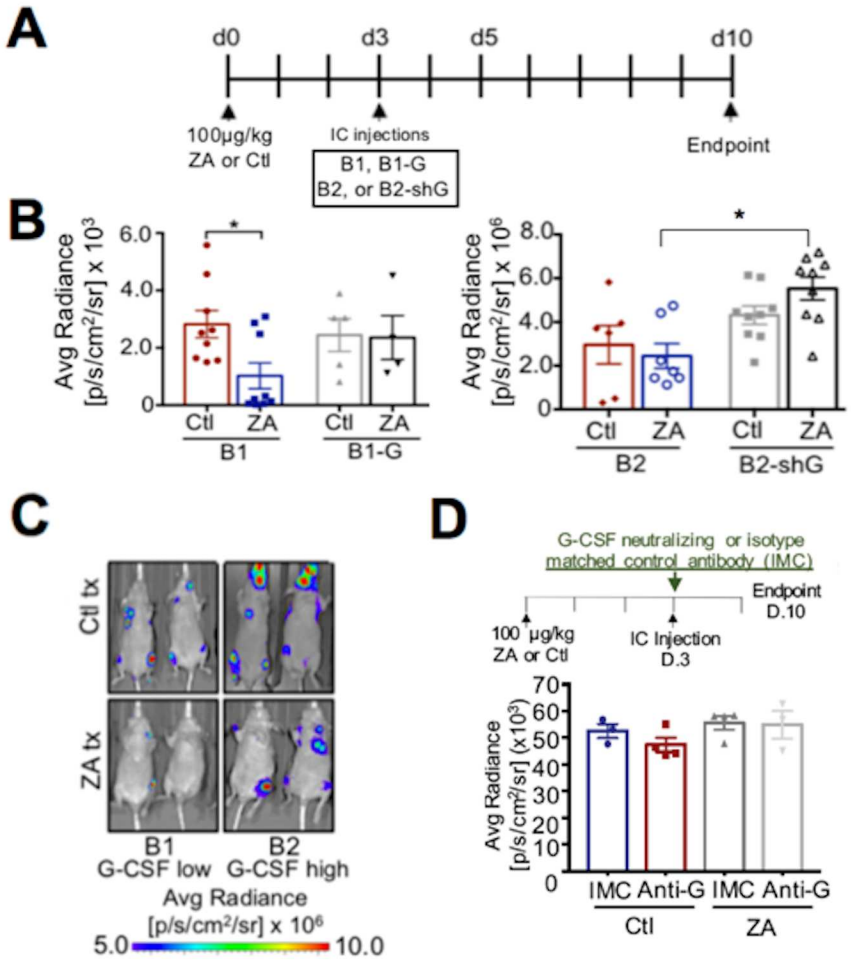

Figure 4

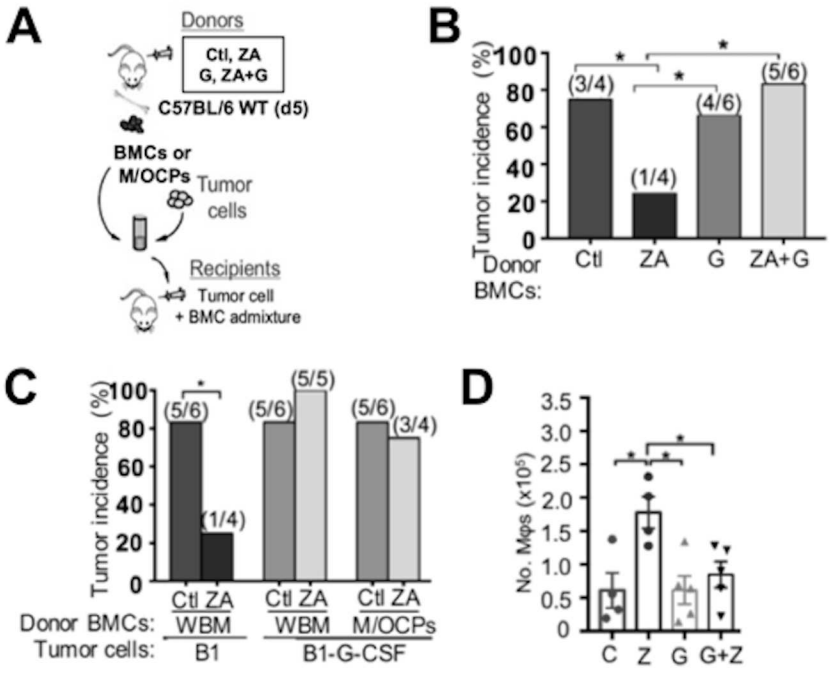

Figure 5

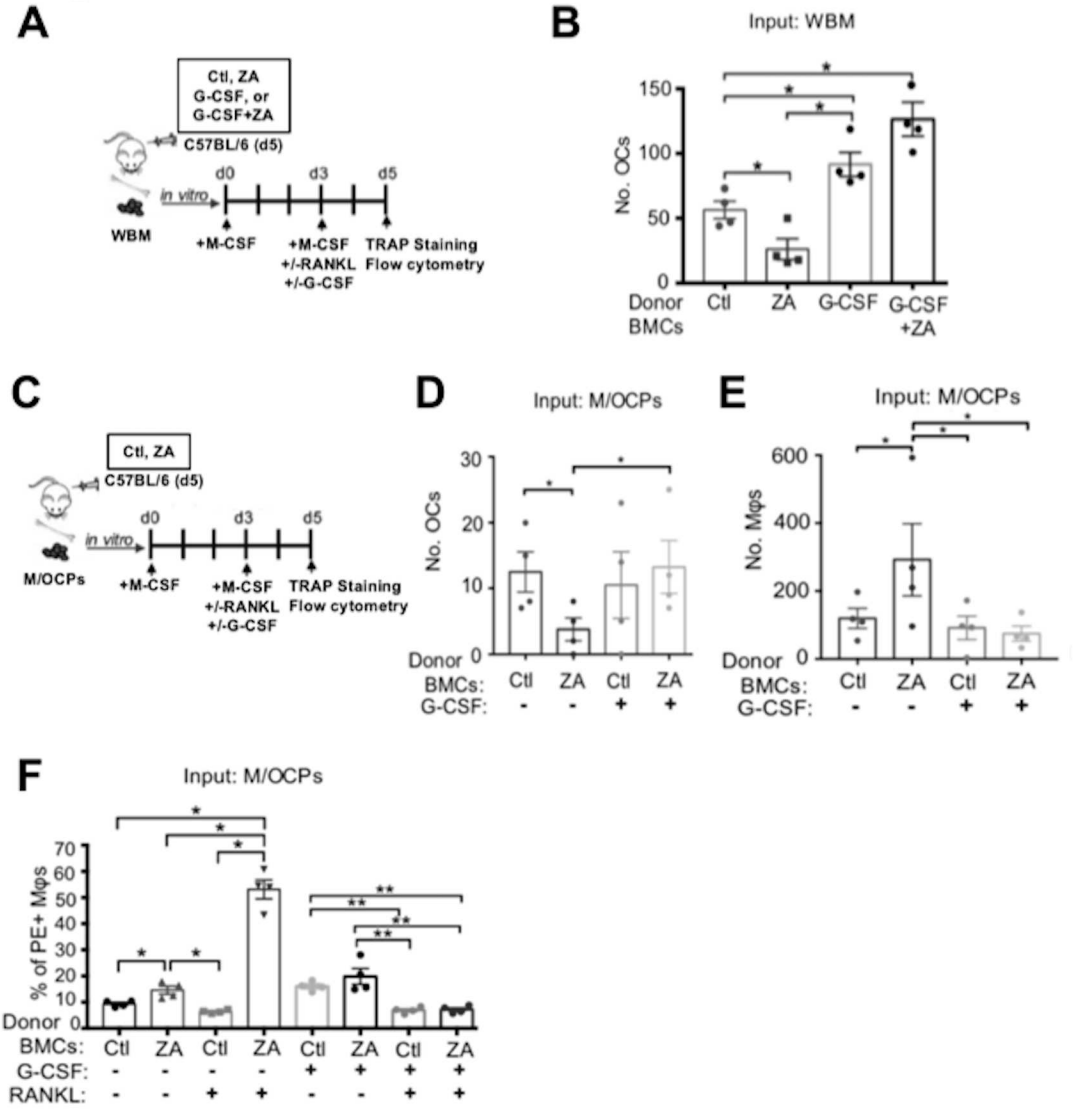

Figure 6

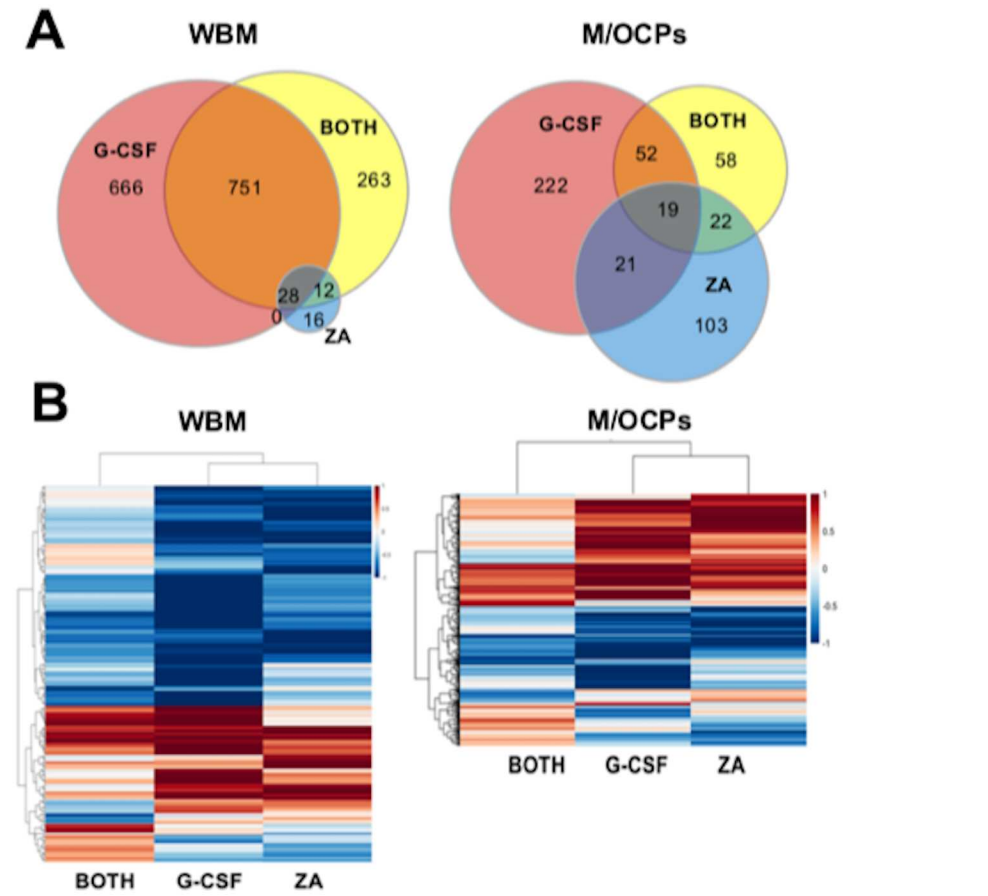

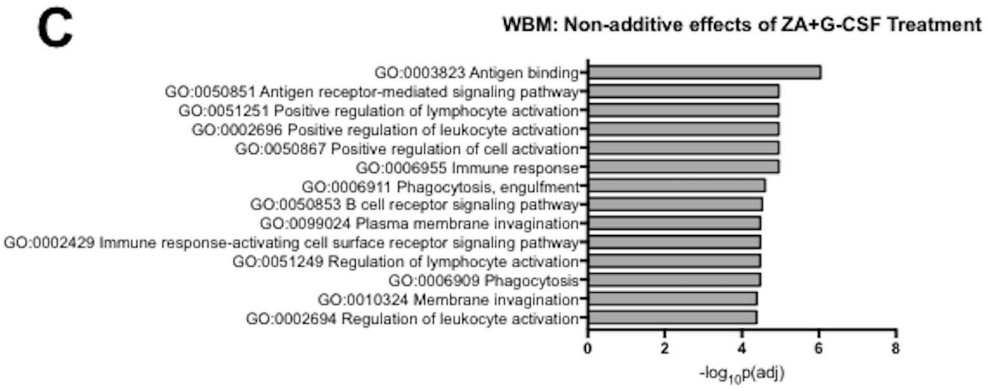

Figure 7

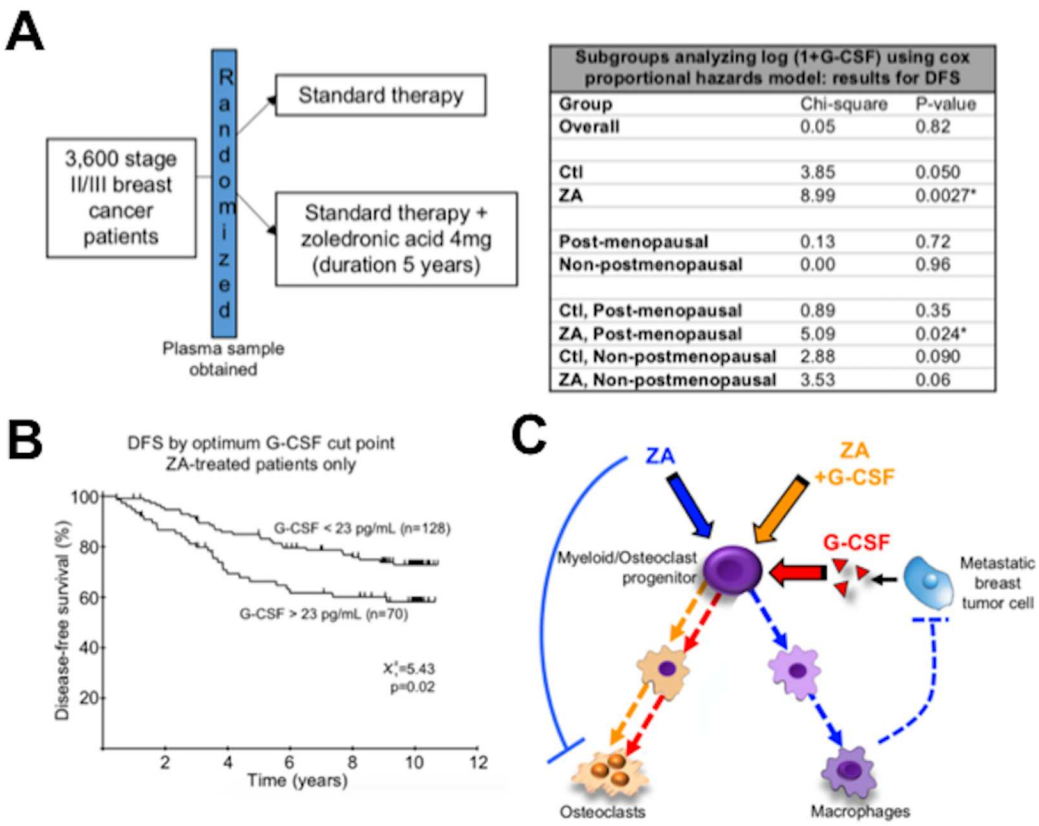

Subgroups analyzing log (1+G-CSF) using cox proportional hazards model: results for DFS		
Group	Chi-square	P-value
Overall	0.05	0.82
Ctl	3.85	0.050
ZA	8.99	0.0027*
Post-menopausal	0.13	0.72
Non-postmenopausal	0.00	0.96
Ctl, Post-menopausal	0.89	0.35
ZA, Post-menopausal	5.09	0.024*
Ctl, Non-postmenopausal	2.88	0.090
ZA, Non-postmenopausal	3.53	0.06

AACR American Association for Cancer Research

Cancer Research

The Journal of Cancer Research (1916–1930) | The American Journal of Cancer (1931–1940)

Modulating bone marrow hematopoietic lineage potential to prevent bone metastasis in breast cancer

Jessalyn M. Ubellacker, Ninib Baryawno, Nicolas Severe, et al.

Cancer Res Published OnlineFirst July 31, 2018.